

Determination of the $D^0 \rightarrow K^- \pi^+ \pi^0$ and $D^0 \rightarrow K^- \pi^+ \pi^+ \pi^-$ Coherence Factors and Average Strong-Phase Differences Using Quantum-Correlated Measurements

N. Lowrey,¹ S. Mehrabyan,¹ M. Selen,¹ J. Wiss,¹ R. E. Mitchell,² M. R. Shepherd,²
D. Besson,³ T. K. Pedlar,⁴ D. Cronin-Hennessy,⁵ K. Y. Gao,⁵ J. Hietala,⁵ Y. Kubota,⁵
T. Klein,⁵ R. Poling,⁵ A. W. Scott,⁵ P. Zweber,⁵ S. Dobbs,⁶ Z. Metreveli,⁶ K. K. Seth,⁶
B. J. Y. Tan,⁶ A. Tomaradze,⁶ J. Libby,⁷ L. Martin,⁷ N. Harnew,⁷ A. Powell,⁷
G. Wilkinson,⁷ H. Mendez,⁸ J. Y. Ge,⁹ D. H. Miller,⁹ I. P. J. Shipsey,⁹ B. Xin,⁹
G. S. Adams,¹⁰ D. Hu,¹⁰ B. Moziak,¹⁰ J. Napolitano,¹⁰ K. M. Ecklund,¹¹ Q. He,¹²
J. Insler,¹² H. Muramatsu,¹² C. S. Park,¹² E. H. Thorndike,¹² F. Yang,¹² M. Artuso,¹³
S. Blusk,¹³ S. Khalil,¹³ J. Li,¹³ R. Mountain,¹³ K. Randrianarivony,¹³ N. Sultana,¹³
T. Skwarnicki,¹³ S. Stone,¹³ J. C. Wang,¹³ L. M. Zhang,¹³ T. Gershon,¹⁴ G. Bonvicini,¹⁵
D. Cinabro,¹⁵ M. Dubrovin,¹⁵ A. Lincoln,¹⁵ M. J. Smith,¹⁵ P. Zhou,¹⁵ J. Zhu,¹⁵ P. Naik,¹⁶
J. Rademacker,¹⁶ D. M. Asner,¹⁷ K. W. Edwards,¹⁷ J. Reed,¹⁷ A. N. Robichaud,¹⁷
G. Tatishvili,¹⁷ E. J. White,¹⁷ R. A. Briere,¹⁸ H. Vogel,¹⁸ P. U. E. Onyisi,¹⁹ J. L. Rosner,¹⁹
J. P. Alexander,²⁰ D. G. Cassel,²⁰ J. E. Duboscq,^{20,*} R. Ehrlich,²⁰ L. Fields,²⁰
L. Gibbons,²⁰ R. Gray,²⁰ S. W. Gray,²⁰ D. L. Hartill,²⁰ B. K. Heltsley,²⁰ D. Hertz,²⁰
J. M. Hunt,²⁰ J. Kandaswamy,²⁰ D. L. Kreinick,²⁰ V. E. Kuznetsov,²⁰ J. Ledoux,²⁰
H. Mahlke-Krüger,²⁰ J. R. Patterson,²⁰ D. Peterson,²⁰ D. Riley,²⁰ A. Ryd,²⁰ A. J. Sadoff,²⁰
X. Shi,²⁰ S. Stroiney,²⁰ W. M. Sun,²⁰ T. Wilksen,²⁰ J. Yelton,²¹ and P. Rubin²²

(CLEO Collaboration)

¹*University of Illinois, Urbana-Champaign, Illinois 61801, USA*

²*Indiana University, Bloomington, Indiana 47405, USA*

³*University of Kansas, Lawrence, Kansas 66045, USA*

⁴*Luther College, Decorah, Iowa 52101, USA*

⁵*University of Minnesota, Minneapolis, Minnesota 55455, USA*

⁶*Northwestern University, Evanston, Illinois 60208, USA*

⁷*University of Oxford, Oxford OX1 3RH, UK*

⁸*University of Puerto Rico, Mayaguez, Puerto Rico 00681*

⁹*Purdue University, West Lafayette, Indiana 47907, USA*

¹⁰*Rensselaer Polytechnic Institute, Troy, New York 12180, USA*

¹¹*Rice University, Houston, TX 77005, USA*

¹²*University of Rochester, Rochester, New York 14627, USA*

¹³*Syracuse University, Syracuse, New York 13244, USA*

¹⁴*University of Warwick, Coventry CV4 7AL, United Kingdom*

¹⁵*Wayne State University, Detroit, Michigan 48202, USA*

¹⁶*University of Bristol, Bristol BS8 1TL, UK*

¹⁷*Carleton University, Ottawa, Ontario, Canada K1S 5B6*

¹⁸*Carnegie Mellon University, Pittsburgh, Pennsylvania 15213, USA*

¹⁹*Enrico Fermi Institute, University of Chicago, Chicago, Illinois 60637, USA*

²⁰*Cornell University, Ithaca, New York 14853, USA*

²¹*University of Florida, Gainesville, Florida 32611, USA*

²²*George Mason University, Fairfax, Virginia 22030, USA*

(Dated: October 3, 2018)

Abstract

The first measurements of the coherence factors ($R_{K\pi\pi^0}$ and $R_{K3\pi}$) and the average strong-phase differences ($\delta_D^{K\pi\pi^0}$ and $\delta_D^{K3\pi}$) for $D^0 \rightarrow K^-\pi^+\pi^0$ and $D^0 \rightarrow K^-\pi^+\pi^+\pi^-$ are presented. These parameters can be used to improve the determination of the unitarity triangle angle γ in $B^- \rightarrow DK^-$ decays, where D is a D^0 or \bar{D}^0 meson decaying to the same final state. The measurements are made using quantum-correlated, fully-reconstructed $D^0\bar{D}^0$ pairs produced in e^+e^- collisions at the $\psi(3770)$ resonance. The measured values are: $R_{K\pi\pi^0} = 0.84 \pm 0.07$, $\delta_D^{K\pi\pi^0} = (227_{-17}^{+14})^\circ$, $R_{K3\pi} = 0.33_{-0.23}^{+0.20}$, and $\delta_D^{K3\pi} = (114_{-23}^{+26})^\circ$. These results indicate significant coherence in the decay $D^0 \rightarrow K^-\pi^+\pi^0$, whereas lower coherence is observed in the decay $D^0 \rightarrow K^-\pi^+\pi^+\pi^-$. The analysis also results in a small improvement in the knowledge of other D -meson parameters, in particular the strong-phase difference for $D^0 \rightarrow K^-\pi^+$, $\delta_D^{K\pi}$, and the mixing parameter, y .

*Deceased

This paper presents the first determination of the coherence factors and the average strong-phase differences for $D^0 \rightarrow K^- \pi^+ \pi^0$ and $D^0 \rightarrow K^- \pi^+ \pi^+ \pi^-$ made using quantum-correlated, fully-reconstructed (double-tagged) $D^0 \bar{D}^0$ pairs produced in $e^+ e^-$ collisions at the $\psi(3770)$ resonance. Knowledge of these parameters improves the sensitivity of measurements of the unitarity triangle angle γ using B -meson decays to these D -meson final states. Although CP -violation involving B -mesons has been clearly established experimentally [1], and existing results are in good agreement with Standard Model predictions, additional and improved measurements are required to overconstrain the Cabibbo-Kobayashi-Maskawa (CKM) quark-mixing matrix [2] and probe for the effects of non-Standard Model physics. An important ingredient in this program will be a precise determination of the angle γ .

Several methods to determine γ using $B^- \rightarrow DK^-$ [3] decays have been proposed [4, 5, 6]. Here, D refers to either a D^0 or \bar{D}^0 meson. All these methods exploit the fact that a B^- can decay into $D^0 K^-$ and $\bar{D}^0 K^-$ final states via $b \rightarrow c \bar{u} s$ and $b \rightarrow u \bar{c} s$ transitions, respectively. The weak phase between these two transitions is equal to $-\gamma$. Therefore, the amplitudes are related by: $\mathcal{A}(B^- \rightarrow \bar{D}^0 K^-)/\mathcal{A}(B^- \rightarrow D^0 K^-) = r_B e^{i(\delta_B - \gamma)}$, where $r_B \sim 0.1$ is the absolute amplitude ratio and δ_B is the strong-phase difference. The two amplitudes interfere with one another if the D^0 and \bar{D}^0 decay to the same final state, which can lead to direct CP -violation between the B^- and B^+ decay rates if γ is non-zero.

The Atwood-Dunietz-Soni (ADS) method [5] uses common flavor-specific final states such as $D \rightarrow K^- \pi^+$ to determine γ . The rates are given by:

$$\begin{aligned} \Gamma(B^\mp \rightarrow D(K^\mp \pi^\pm)K^\mp) \\ \propto 1 + (r_B r_D^{K\pi})^2 + 2r_B r_D^{K\pi} \cos(\delta_B - \delta_D^{K\pi} \mp \gamma) \end{aligned} \quad (1)$$

and

$$\begin{aligned} \Gamma(B^\mp \rightarrow D(K^\pm \pi^\mp)K^\mp) \\ \propto (r_B)^2 + (r_D^{K\pi})^2 + 2r_B r_D^{K\pi} \cos(\delta_B + \delta_D^{K\pi} \mp \gamma) \end{aligned} \quad (2)$$

where $r_D^{K\pi}$ is the absolute amplitude ratio of the doubly-Cabibbo-suppressed (DCS) decay $D^0 \rightarrow K^+ \pi^-$ to the Cabibbo-favored (CF) decay $D^0 \rightarrow K^- \pi^+$, and $\delta_D^{K\pi}$ is the strong-phase difference between these two amplitudes, which is defined as: $\mathcal{A}(D^0 \rightarrow K^+ \pi^-)/\mathcal{A}(D^0 \rightarrow K^- \pi^+) = r_D^{K\pi} e^{-i\delta_D^{K\pi}}$. Present measurements give $r_D^{K\pi} = 0.0579 \pm 0.0007$ [7], therefore, the terms on the righthand side of Eq. (2) are all of the same order, which allows significant changes to $\Gamma(B^\mp \rightarrow D(K^\pm \pi^\mp)K^\mp)$ depending on the values of γ and the strong phases. The suppressed decays $B^\mp \rightarrow D(K^\pm \pi^\mp)K^\mp$ have not yet been observed [8, 9]. The measurement of $\delta_D^{K\pi}$ has been made in quantum-correlated $D^0 \bar{D}^0$ decays [10] in a similar manner to the analysis reported in this paper.

The flavor-specific final states $D \rightarrow K^- \pi^+ \pi^+ \pi^-$ ($D \rightarrow K^- 3\pi$) and $D \rightarrow K^- \pi^+ \pi^0$ have significantly larger branching fractions than $D \rightarrow K^- \pi^+$ [11]. However, for three- or four-body D decay the amplitude ratio and strong-phase difference vary over phase space. For such D decays, for example $D \rightarrow K^- \pi^+ \pi^0$, Eq. (2) is modified as follows [12]:

$$\begin{aligned} \Gamma(B^\mp \rightarrow D(K^\pm \pi^\mp \pi^0)K^\mp) \\ \propto (r_B)^2 + (r_D^{K\pi\pi^0})^2 \\ + 2r_B r_D^{K\pi\pi^0} R_{K\pi\pi^0} \cos(\delta_B + \delta_D^{K\pi\pi^0} \mp \gamma), \end{aligned} \quad (3)$$

where $R_{K\pi\pi^0}$, $\delta_{K\pi\pi^0}$ and $r_D^{K\pi\pi^0}$ are defined as:

$$R_{K\pi\pi^0} e^{-i\delta_D^{K\pi\pi^0}} = \frac{\int \mathcal{A}_{K^- \pi^+ \pi^0}(\mathbf{x}) \mathcal{A}_{K^+ \pi^- \pi^0}(\mathbf{x}) d\mathbf{x}}{A_{K^- \pi^+ \pi^0} A_{K^+ \pi^- \pi^0}} \text{ and}$$

$$r_D^{K\pi\pi^0} = \frac{A_{K^+\pi^-\pi^0}}{A_{K^-\pi^+\pi^0}}.$$

Here $\mathcal{A}_{K^\pm\pi^\mp\pi^0}(\mathbf{x})$ is the amplitude for $D^0 \rightarrow K^\pm\pi^\mp\pi^0$ at a point in multi-body phase space described by parameters \mathbf{x} , and $A_{K^\pm\pi^\mp\pi^0}^2 = \int |\mathcal{A}_{K^\pm\pi^\mp\pi^0}(\mathbf{x})|^2 d\mathbf{x}$. (The expressions for $D \rightarrow K^-\pi^+\pi^+\pi^-$ take the same form and involve the parameters $r_D^{K3\pi}$, $R_{K3\pi}$ and $\delta_D^{K3\pi}$.)

The parameter $R_{K\pi\pi^0}$ is known as the coherence factor and can take any value from zero to one. A small value of $R_{K\pi\pi^0}$ indicates a lack of coherence between the intermediate states involved in the decay, a situation expected when there are many resonances contributing; a value close to one occurs when the resonances are largely in phase, or one state dominates. Decays to two-body final states, such as $D^0 \rightarrow K^-\pi^+$, and to CP eigenstates have a coherence factor equal to one. Even if the coherence is small the rate described by Eq. (3) is still useful, because it possesses high sensitivity to the parameter r_B .

The coherence factors R_F and average strong-phase difference, δ_D^F , where $F = K^-\pi^+\pi^0$ or $K^-\pi^+\pi^+\pi^-$, can be determined using double-tagged $D^0\bar{D}^0$ pairs produced in e^+e^- collisions at the $\psi(3770)$ resonance. The two mesons are produced in a C -odd eigenstate and their decays are quantum-correlated. The rate for the two D mesons to decay to states F and G is given by [12]:

$$\begin{aligned} \Gamma(F|G) &= \Gamma_0 \int \int |\mathcal{A}_F(\mathbf{x})\mathcal{A}_{\bar{G}}(\mathbf{y}) - \mathcal{A}_{\bar{F}}(\mathbf{x})\mathcal{A}_G(\mathbf{y})|^2 d\mathbf{x}d\mathbf{y} \\ &= \Gamma_0 [A_F^2 A_{\bar{G}}^2 + A_{\bar{F}}^2 A_G^2 \\ &\quad - 2R_F R_G A_F A_{\bar{F}} A_G A_{\bar{G}} \cos(\delta_D^G - \delta_D^F)], \end{aligned} \quad (4)$$

where $\mathcal{A}_F(\mathbf{x})$ ($\mathcal{A}_{\bar{G}}(\mathbf{y})$) and $\mathcal{A}_{\bar{F}}(\mathbf{x})$ ($\mathcal{A}_{\bar{G}}(\mathbf{y})$) are the amplitudes of $D^0 \rightarrow F$ ($D^0 \rightarrow G$) and $D^0 \rightarrow \bar{F}$ ($D^0 \rightarrow \bar{G}$) at points \mathbf{x} (\mathbf{y}) in phase space, respectively, and $\Gamma_0 = \Gamma(\psi(3770) \rightarrow D^0\bar{D}^0)$. From Eq. (4) the following double-tagged rates arise:

$$\begin{aligned} \Gamma(F|CP) &= \Gamma_0 A_F^2 A_{CP}^2 [1 + (r_D^F)^2 \\ &\quad - 2\lambda_\pm r_D^F R_F \cos \delta_D^F], \end{aligned} \quad (5)$$

$$\Gamma(F|F) = \Gamma_0 A_F^2 A_{\bar{F}}^2 [1 - R_F^2], \quad (6)$$

$$\begin{aligned} \Gamma(F|K^-\pi) &= \Gamma_0 A_F^2 A_{K^-\pi^+}^2 [(r_D^{K\pi})^2 + (r_D^F)^2 \\ &\quad - 2r_D^{K\pi} r_D^F R_F \cos(\delta_D^{K\pi} - \delta_D^F)] \end{aligned} \quad (7)$$

and

$$\begin{aligned} \Gamma(K^\mp\pi^\pm\pi^0|K^\mp\pi^\pm\pi^\pm\pi^\mp) \\ &= \Gamma_0 A_{K^-\pi^+\pi^0}^2 A_{K^-\pi^+\pi^+\pi^-}^2 [(r_D^{K3\pi})^2 + (r_D^{K\pi\pi^0})^2 \\ &\quad - 2r_D^{K3\pi} r_D^{K\pi\pi^0} R_{K3\pi} R_{K\pi\pi^0} \cos(\delta_D^{K3\pi} - \delta_D^{K\pi\pi^0})]. \end{aligned} \quad (8)$$

Here CP denotes a CP eigenstate with eigenvalue $\lambda_\pm = \pm 1$. The final states described by Eqs. (6), (7), and (8) are referred to as ‘like-sign’ (LS) on account of the charges of the two kaons involved. Furthermore, the following relations are noted: $\Gamma(F|CP) = \Gamma(\bar{F}|CP)$, $\Gamma(F|F) = \Gamma(\bar{F}|\bar{F})$ and $\Gamma(F|K^-\pi^+) = \Gamma(\bar{F}|K^+\pi^-)$; these expressions ignore CP -violation in D decay, which is well motivated theoretically and by current experimental limits [13].

To relate the amplitudes in Eqs. (5) to (8) to branching fractions the effects of charm mixing must be included. Charm mixing is commonly characterised by the parameters $x = (M_+ - M_-)/\Gamma$ and $y = (\Gamma_+ - \Gamma_-)/2\Gamma$, where M_\pm and Γ_\pm are the masses and widths of the $\lambda_\pm = \pm 1$ neutral D meson mass eigenstates, respectively, and $\Gamma = (\Gamma_+ + \Gamma_-)/2$.

The relations between amplitudes and branching fractions, following Ref. [14], are given in Table I.

The best constraints on x , y and $\delta_D^{K\pi}$ come from the combination of several measurements [13]. These constraints [7] are included in the analysis reported here to improve the determination of R_F and δ_D^F . However, the analysis is also sensitive to these parameters so results are presented without the external constraints as well.

TABLE I: Relations between branching fractions, \mathcal{B} , and amplitudes including the effects of charm mixing. The DCS and CP expressions are quoted to $\mathcal{O}((x/r_D)^2, (y/r_D)^2)$ and $\mathcal{O}(y)$, respectively. The corrections due to mixing in the CF amplitude are negligible ($< 1\%$).

Mode	\mathcal{B}
$D^0 \rightarrow CP$	$A_{CP}^2(1 - \lambda_{\pm}y)$
$D^0 \rightarrow F$	A_F^2
$D^0 \rightarrow \bar{F}$	$A_{\bar{F}}^2[1 - (y/r_D^F) R_F \cos \delta_D^F$ $+ (x/r_D^F) R_F \sin \delta_D^F + (y^2 + x^2)/2(r_D^F)^2]$
$D^0 \rightarrow K^-\pi^+$	$A_{K^-\pi^+}^2$
$D^0 \rightarrow K^+\pi^-$	$A_{K^+\pi^-}^2[1 - (y/r_D^{K\pi}) \cos \delta_D^{K\pi}$ $+ (x/r_D^{K\pi}) \sin \delta_D^{K\pi} + (y^2 + x^2)/2(r_D^{K\pi})^2]$

An 818 pb $^{-1}$ data set of e^+e^- collisions produced by the Cornell Electron Storage Ring (CESR) at $E_{\text{cm}} = 3.77$ GeV and collected with the CLEO-c detector is analysed. The CLEO-c detector is described in detail elsewhere [15]. Table II lists the reconstructed D^0 and \bar{D}^0 final states, with $\pi^0 \rightarrow \gamma\gamma$, $K_S^0 \rightarrow \pi^+\pi^-$, $\omega \rightarrow \pi^+\pi^-\pi^0$, $\phi \rightarrow K^+K^-$, $\eta \rightarrow \gamma\gamma$, $\eta \rightarrow \pi^+\pi^-\pi^0$ and $\eta' \rightarrow \eta(\gamma\gamma)\pi^+\pi^-$. When required in the analysis, reconstruction efficiencies are calculated from simulated samples of signal D decays. Backgrounds from other $D\bar{D}$ decays are estimated from a simulated sample of generic $D\bar{D}$ decays.

TABLE II: D final states reconstructed in this analysis.

Type	Final states
Flavored	$K^{\mp}\pi^{\pm}, K^{\mp}\pi^{\pm}\pi^{\pm}\pi^{\mp}, K^{\mp}\pi^{\pm}\pi^0$
CP -even	$K^+K^-, \pi^+\pi^-, K_S^0\pi^0\pi^0, K_L^0\pi^0, K_L^0\omega$
CP -odd	$K_S^0\pi^0, K_S^0\omega, K_S^0\phi, K_S^0\eta, K_S^0\eta'$

The π_0 , K_S^0 , ω and $\eta \rightarrow \gamma\gamma$ reconstruction is identical to that used in Ref. [10]. Candidates for $\eta \rightarrow \pi^+\pi^-\pi^0$, η' , and ϕ mesons are considered if their masses are within the intervals [506, 590] MeV/ c^2 , [950, 964] MeV/ c^2 , and [1009, 1033] MeV/ c^2 , respectively. Final states that do not contain a K_L^0 meson are fully reconstructed via two kinematic variables: the beam-constrained candidate mass, $M_{bc} \equiv \sqrt{E_{\text{cm}}^2/(4c^4) - \mathbf{p}_D^2/c^2}$, where \mathbf{p}_D is the D candidate momentum, and $\Delta E \equiv E_D - E_{\text{cm}}/2$, where E_D is the sum of the D daughter candidate energies. The double-tagged yield is determined from counting events in signal and sideband regions of M_{bc} . Fig. 1 (a) shows the distribution of M_{bc} for $D \rightarrow K^-\pi^+\pi^0$ candidates tagged by $D \rightarrow K_S^0\pi^0$ decays for data and simulated background events. The selection and yield determination procedures are similar to those presented in Ref. [10]. For modes that were not considered in Ref. [10] the values of the ΔE criteria are identical to those used in Ref. [16]. In

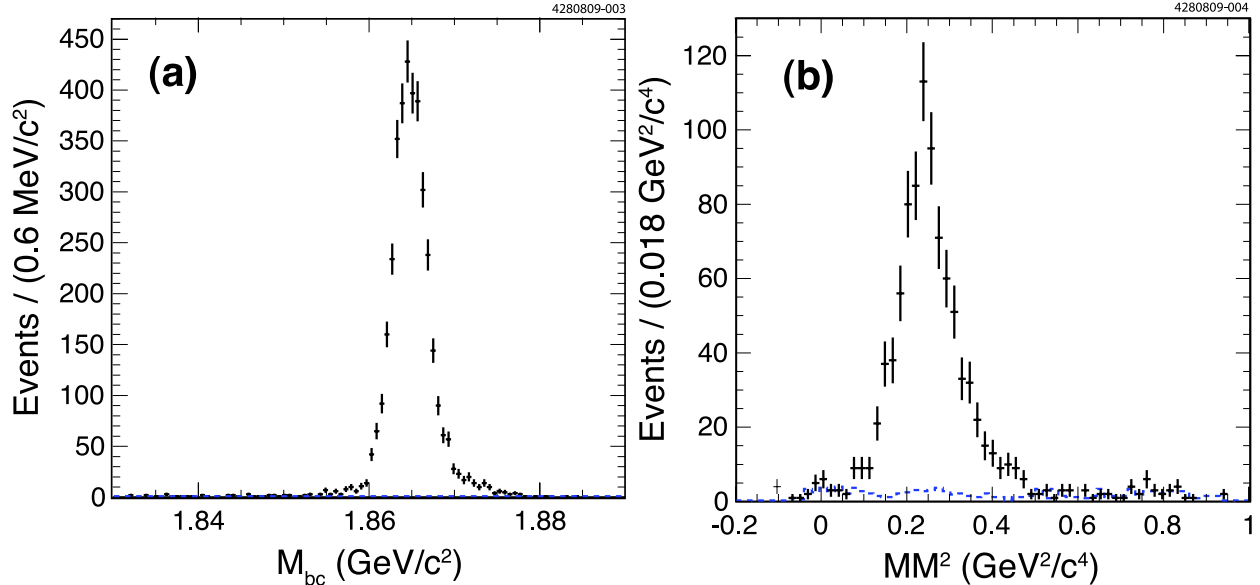


FIG. 1: Distributions of (a) M_{bc} for $D \rightarrow K^- \pi^+ \pi^0$ candidates tagged by $D \rightarrow K_S^0 \pi^0$ and (b) missing-mass squared for $D \rightarrow K_L^0 \pi^0$ tagged $D \rightarrow K3\pi$ candidates for data (points) and expected background (dotted line).

addition, to suppress background from $D^0 \rightarrow K_S^0 K^\pm \pi^\mp$ to $D^0 \rightarrow K^\pm \pi^\mp \pi^\mp \pi^\pm$, requirements are placed on the $\pi^+ \pi^-$ pairs to be consistent with originating from the $e^+ e^-$ collision point. Furthermore, in events where $K^- 3\pi$ or $K^- \pi^+ \pi^0$ are tagged by $K^\pm \pi^\mp$, at least one of the daughters of the two-body decay is required to be in the acceptance of the Ring Imaging Cherenkov detector; this criterion suppresses events where $K^- \pi^+$ is misidentified as $K^+ \pi^-$.

To identify CP -tags containing a single K_L^0 meson, we compute the missing-mass recoiling against the signal D candidate and the sister particles in the assumed tag decay, and select events consistent with the mass of the K_L^0 meson squared [17]. Yields are extracted from the signal and sideband regions of the missing-mass distribution. Fig. 1 (b) is the distribution of missing-mass squared for $D \rightarrow K3\pi$ candidates tagged by $D \rightarrow K_L^0 \pi^0$ decays for data and simulated background.

Significant peaking backgrounds arise in a few modes: non-resonant decays to $\pi^+ \pi^- \pi^0$ for modes reconstructed including an ω or $\eta \rightarrow \pi^+ \pi^- \pi^0$, $D \rightarrow K_S^0(\pi^0 \pi^0)X$ misidentified as $D \rightarrow K_L^0 X$ decays, and $D \rightarrow K_S^0(\pi^+ \pi^-)K^- \pi^+$ to $D \rightarrow K^- 3\pi$. However, these backgrounds are all smaller than the statistical uncertainty on the yields. The peaking background yields are estimated from a simulated sample with a size equivalent to approximately 3.3 times the data sample; the uncertainty on the peaking background yield is that due to the statistics of this sample. This uncertainty is added in quadrature to that on the combinatoric background subtracted signal yields. There is a further peaking background of $D \rightarrow K^+ \pi^-$ decays misidentified as $D \rightarrow K^- \pi^+$ for the like-sign $K^- 3\pi$ or $K^- \pi^+ \pi^0$ tagged by $K^\pm \pi^\mp$, which is also estimated from simulated sample. However, this contamination is treated as a separate source of systematic uncertainty because it is the dominant source for some measurements. The measured event yields after background subtraction are given in Table III.

The results of the analysis are presented in terms of the observables $\rho_{CP^\pm}^F$, ρ_{LS}^F , $\rho_{K\pi,LS}^F$ and $\rho_{K3\pi,LS}^{K\pi\pi^0}$, which are the ratios of the measured values of $\Gamma(F|CP)$, $\Gamma(F|F)$, $\Gamma(F|K^- \pi^+)$ and $\Gamma(K^\mp \pi^\pm \pi^0 | K^\mp \pi^\pm \pi^\pm \pi^\mp)$ to the expected rates, on the assumption that the two D mesons

TABLE III: Measured double-tagged signal yields.

Mode	$K^\pm\pi^\mp\pi^\mp\pi^\pm$	$K^\pm\pi^\mp\pi^0$	$K^\pm\pi^\mp$
$K^\mp\pi^\pm\pi^\pm\pi^\mp$	$4,044 \pm 64$	–	–
$K^\pm\pi^\mp\pi^\mp\pi^\pm$	29.1 ± 5.9	–	–
$K^\mp\pi^\pm\pi^0$	$9,594 \pm 99$	$7,342 \pm 87$	–
$K^\pm\pi^\mp\pi^0$	63.6 ± 8.8	12.5 ± 4.1	–
$K^\mp\pi^\pm$	$5,206 \pm 72$	$7,155 \pm 85$	–
$K^\pm\pi^\mp$	35.6 ± 6.2	7.3 ± 3.3	–
K^+K^-	536 ± 23	764 ± 28	–
$\pi^+\pi^-$	246 ± 16	336 ± 18	–
$K_S^0\pi^0\pi^0$	283 ± 18	406 ± 21	221 ± 15
$K_L^0\pi^0$	827 ± 30	$1,236 \pm 38$	689 ± 28
$K_L^0\omega$	296 ± 18	449 ± 22	251 ± 17
$K_S^0\pi^0$	705 ± 27	891 ± 30	473 ± 22
$K_S^0\omega$	319 ± 19	389 ± 21	183 ± 14
$K_S^0\phi$	53.0 ± 7.5	90.9 ± 9.9	42.8 ± 6.9
$K_S^0\eta(\gamma\gamma)$	128 ± 12	116 ± 11	65.5 ± 8.3
$K_S^0\eta(\pi^+\pi^-\pi^0)$	35.9 ± 6.5	36.3 ± 7.2	27.2 ± 5.4
$K_S^0\eta'$	35.7 ± 6.0	60.6 ± 7.8	30.0 ± 5.5

decay in an uncorrelated fashion or have zero coherence. Therefore significant deviation of any of the ρ parameters from a value of one can only come about through the quantum-correlated nature of $D\bar{D}$ production at the $\psi(3770)$ and a non-zero coherence in the D decay. The ρ observables are related to the background and efficiency corrected signal yields, S , as follows:

$$\rho_{LS}^F = \frac{S(F|F) + S(\bar{F}|\bar{F})}{2N_{D^0\bar{D}^0}\mathcal{B}(D^0 \rightarrow F)\mathcal{B}(D^0 \rightarrow \bar{F})}, \quad (9)$$

$$\rho_{K\pi,LS}^F = \frac{[S(F|K^-\pi^+) + S(\bar{F}|K^+\pi^-)]}{2N_{D^0\bar{D}^0}[\mathcal{B}(D^0 \rightarrow F)\mathcal{B}(D^0 \rightarrow K^+\pi^-) + \mathcal{B}(D^0 \rightarrow \bar{F})\mathcal{B}(D^0 \rightarrow K^-\pi^+)]}, \quad (10)$$

$$\rho_{CP\pm}^F = \frac{[S(F|CP) + S(\bar{F}|CP)]}{2N_{D^0\bar{D}^0}\mathcal{B}(D^0 \rightarrow CP) [\mathcal{B}(D^0 \rightarrow F) + \mathcal{B}(D^0 \rightarrow \bar{F})]}, \quad (11)$$

and

$$\rho_{K3\pi,LS}^{K\pi\pi^0} = \frac{[S(K^-\pi^+\pi^0|K^-3\pi) + S(K^+\pi^-\pi^0|K^+3\pi)]}{2N_{D^0\bar{D}^0}[\mathcal{B}(D^0 \rightarrow K^-\pi^+\pi^0)\mathcal{B}(D^0 \rightarrow K^+3\pi) + \mathcal{B}(D^0 \rightarrow K^+\pi^-\pi^0)\mathcal{B}(D^0 \rightarrow K^-3\pi)]}, \quad (12)$$

where $N_{D^0\bar{D}^0}$ is the total number of $\psi(3770) \rightarrow D^0\bar{D}^0$ events.

In the extraction of each like-sign observable, the product of $N_{D^0\bar{D}^0}$ and the reconstruction efficiency is determined from the background-subtracted yield in the corresponding opposite-sign samples, taking the values of the branching fractions reported in Ref. [11]. For example,

in the case of ρ_{LS}^F , the observable is given by

$$\rho_{LS}^F = \frac{N(F|F) + N(\bar{F}|\bar{F})}{2N(F|\bar{F})} \frac{\mathcal{B}(D^0 \rightarrow F)}{\mathcal{B}(D^0 \rightarrow \bar{F})}, \quad (13)$$

where N are the background-subtracted yields without any efficiency corrections applied. For the majority of the CP double-tags an alternative normalization procedure is exploited, whereby knowledge of $N_{D^0\bar{D}^0}$, the reconstruction efficiency and the branching ratio of the CP mode, which in many cases is poorly known, is accommodated by a comparison with double-tag events involving the CP -tag against $D \rightarrow K^-\pi^+$ decays. The good knowledge of $\delta_D^{K\pi}$ [7, 10, 18] allows the contribution from quantum-correlations in these normalization events to be accounted for. Small corrections are applied related to the differing environment in which the tag is reconstructed in $K^-\pi^+$, $K^-\pi^+\pi^0$ and $K^-\pi^+\pi^-\pi^+$ events. In the case of the tags K^+K^- and $\pi^+\pi^-$ the branching ratios are known well enough to use the values directly from Ref. [11], together with measurements of the reconstruction efficiency and $S(F|K^+\pi^-)$.

Table IV shows the measured value of each observable. In the case of $\rho_{CP\pm}^F$ the results from the individual CP -tags are found to be consistent and are therefore combined into mean values for CP -even and CP -odd, taking full account of the correlations among the assigned systematic uncertainties. The most important systematic uncertainties are those arising from the finite size of the $K^-\pi^+$ vs. CP double-tag samples (0.018), residual corrections associated with this normalization procedure (0.008), and knowledge of the CF $D^0 \rightarrow K^-\pi^+\pi^-\pi^+$ and $D^0 \rightarrow K^-\pi^+\pi^0$ branching ratios (0.010). For the $\rho_{LS}^{K3\pi}$ ($\rho_{LS}^{K\pi\pi^0}$) observable the dominant uncertainty of 0.082 (0.021) comes from the knowledge of the DCS branching ratio; this is also a significant component for $\rho_{K\pi,LS}^{K3\pi}$ ($\rho_{K\pi,LS}^{K\pi\pi^0}$), where the uncertainty is 0.034 (0.003), with further important contributions arising from the knowledge of the $D^0 \rightarrow K^+\pi^-$ branching ratio of 0.024 (0.005) and the rate of misidentification of $D^0 \rightarrow K^-\pi^+$ as $D^0 \rightarrow K^+\pi^-$ of 0.016 (0.026). For $\rho_{K3\pi,LS}^{K\pi\pi^0}$ the largest uncertainty is 0.065 from the DCS branching fractions. For all observables uncertainties are also assigned to account for non-uniform acceptance across phase-space; this uncertainty is only found to be significant for $\rho_{LS}^{K3\pi}$, $\rho_{K\pi,LS}^{K3\pi}$ and $\rho_{K3\pi,LS}^{K\pi\pi^0}$ where it is 0.051, 0.040 and 0.037, respectively. The results in Table IV suggest significant coherence in the $D \rightarrow K^-\pi^+\pi^0$ decay, but much less so in the case of $D \rightarrow K^-\pi^+\pi^-\pi^+$.

The relationships between the like-sign kaon observables and the physics parameters are given by:

$$\rho_{LS}^F = \frac{1 - R_F^2}{1 + \frac{(x^2+y^2)}{2(r_D^F)^2} - \frac{R_F}{r_D^F}(y \cos \delta_D^F - x \sin \delta_D^F)}, \quad (14)$$

$$\rho_{K\pi,LS}^F = \frac{[1 + (\frac{r^F}{r_{K\pi}})^2 - 2\frac{r^F}{r_{K\pi}}R_F \cos(\delta_D^{K\pi} - \delta_D^F)]B_{K\pi,LS}^F}{1 + \frac{(x^2+y^2)}{2(r_D^{K\pi})^2} - \frac{1}{r_D^{K\pi}}(y \cos \delta_D^{K\pi} - x \sin \delta_D^{K\pi})}, \quad (15)$$

and

$$\rho_{K3\pi,LS}^{K\pi\pi^0} = \frac{[1 + (\frac{r^{K\pi\pi^0}}{r_{K3\pi}})^2 - 2\frac{r^{K\pi\pi^0}}{r_{K3\pi}}R_{K\pi\pi^0}R_{K3\pi} \cos(\delta_D^{K\pi\pi^0} - \delta_D^{K3\pi})]B_{K3\pi,LS}^{K\pi\pi^0}}{1 + \frac{(x^2+y^2)}{2(r_D^{K3\pi})^2} - \frac{R_{K3\pi}}{r_D^{K3\pi}}(y \cos \delta_D^{K3\pi} - x \sin \delta_D^{K3\pi})}, \quad (16)$$

TABLE IV: Measured ρ observables, where the first uncertainty is statistical and the second systematic.

Observable	Measured Value
$\rho_{CP+}^{K3\pi}$	$1.077 \pm 0.024 \pm 0.029$
$\rho_{CP-}^{K3\pi}$	$0.933 \pm 0.027 \pm 0.046$
$\rho_{LS}^{K3\pi}$	$1.112 \pm 0.226 \pm 0.102$
$\rho_{K\pi,LS}^{K3\pi}$	$0.971 \pm 0.169 \pm 0.062$
$\rho_{CP+}^{K\pi\pi^0}$	$1.073 \pm 0.020 \pm 0.035$
$\rho_{CP-}^{K\pi\pi^0}$	$0.868 \pm 0.023 \pm 0.049$
$\rho_{LS}^{K\pi\pi^0}$	$0.388 \pm 0.127 \pm 0.026$
$\rho_{K\pi,LS}^{K\pi\pi^0}$	$0.170 \pm 0.072 \pm 0.027$
$\rho_{K3\pi,LS}^{K\pi\pi^0}$	$1.221 \pm 0.169 \pm 0.080$

where $B_{K\pi,LS}^F = \mathcal{B}(D^0 \rightarrow F)\mathcal{B}(D^0 \rightarrow K^+\pi^-)/(\mathcal{B}(D^0 \rightarrow F)\mathcal{B}(D^0 \rightarrow K^+\pi^-) + \mathcal{B}(D^0 \rightarrow \bar{F})\mathcal{B}(D^0 \rightarrow K^-\pi^+))$ and $B_{K3\pi,LS}^{K\pi\pi^0} = \mathcal{B}(D^0 \rightarrow K^-\pi^+\pi^0)\mathcal{B}(D^0 \rightarrow K^+3\pi)/(\mathcal{B}(D^0 \rightarrow K^-\pi^+\pi^0)\mathcal{B}(D^0 \rightarrow K^+3\pi) + \mathcal{B}(D^0 \rightarrow K^+\pi^-\pi^0)\mathcal{B}(D^0 \rightarrow K^-3\pi))$.

In making use of the $\rho_{CP\pm}^F$ observables it is convenient to define the CP -invariant observable, Δ_{CP}^F :

$$\Delta_{CP}^F \equiv \lambda_{\pm}(\rho_{CP\pm}^F - 1) = y - 2r_D^F R_F \cos \delta_D^F. \quad (17)$$

Some anticorrelated systematic uncertainties on ρ_{CP+}^F and ρ_{CP-}^F cancel when computing Δ_{CP}^F . It is found that $\Delta_{CP}^{K3\pi} = 0.077 \pm 0.018 \pm 0.022$ and $\Delta_{CP}^{K\pi\pi^0} = 0.097 \pm 0.015 \pm 0.023$, with $\chi^2/d.o.f$ values of 7.3/10 and 5.7/10, respectively.

The values of $R_{K\pi\pi^0}$, $R_{K3\pi}$, $\delta_D^{K\pi\pi^0}$ and $\delta_D^{K3\pi}$ are obtained by a χ^2 fit to ρ_{LS}^F , $\rho_{K\pi,LS}^F$, $\rho_{K\pi\pi^0,LS}^{K3\pi}$ and Δ_{CP}^F . In addition, the fit has x , y , δ_D and the CF and DCS branching fractions for $D \rightarrow K^-\pi^+$, $K^-\pi^+\pi^0$ and $K^-3\pi$ as free parameters. The values of the D -mixing parameters and branching fractions are constrained to those reported in Refs. [7] and [11], respectively; this procedure is referred to as the mixing-constrained fit. The values of the constraints are given in Table V. Correlations amongst all free parameters are accounted for. The results of the mixing-constrained fit are given in Tab. V. The best fit values of the coherence factors and average strong-phase differences are: $R_{K\pi\pi^0} = 0.84 \pm 0.07$, $\delta_D^{K\pi\pi^0} = (227_{-17}^{+14})^\circ$, $R_{K3\pi} = 0.33_{-0.23}^{+0.20}$, and $\delta_D^{K3\pi} = (114_{-23}^{+26})^\circ$. There are also small improvements in the precision of $\delta_D^{K\pi}$, y and the DCS and CF $D \rightarrow K^-3\pi$ branching fractions compared to the external constraints. The uncertainties are those arising from the statistical and systematic uncertainties on the observables. The $\chi^2/d.o.f$ for the mixing-constrained fit is 7.3/3. The correlations amongst the parameters are presented in Ref. [19].

Figures 2(a) and 2(b) show the 1σ , 2σ and 3σ allowed regions of $(R_{K\pi\pi^0}, \delta_D^{K\pi\pi^0})$ and $(R_{K3\pi}, \delta_D^{K3\pi})$ parameter space from the mixing-constrained fit, respectively. The likelihood is computed as $\mathcal{L} = e^{-(\chi^2 - \chi_{\min}^2)/2}$ at a point in parameter space; the fit is repeated at each point with the values of R_F and δ_D^F fixed. The 95% confidence level (CL) intervals for the parameters are found by integrating one-dimensional likelihood scans within the physically allowed region. The following 95% CL intervals are found: $0.70 < R_{K\pi\pi^0} < 0.95$, $167^\circ < \delta_D^{K\pi\pi^0} < 249^\circ$ and $R_{K3\pi} < 0.62$. There is no bound on $\delta_D^{K3\pi}$ at the 95% CL.

The fit is repeated with the constraints on x , y and $\delta_{K\pi}$ removed to estimate these pa-

TABLE V: Results of the mixing-constrained and unconstrained fits to the observables. Values of external constraints are listed. The uncertainties are those arising from the statistical and systematic uncertainties on the observables.

Parameter	Mixing constrained	Mixing unconstrained	External input
$R_{K\pi\pi^0}$	0.84 ± 0.07	$0.78^{+0.11}_{-0.25}$	–
$\delta_D^{K\pi\pi^0}$ (°)	227^{+14}_{-17}	239^{+32}_{-28}	–
$R_{K3\pi}$	$0.33^{+0.26}_{-0.23}$	$0.36^{+0.24}_{-0.30}$	–
$\delta_D^{K3\pi}$ (°)	114^{+26}_{-23}	118^{+62}_{-53}	–
x (%)	0.96 ± 0.25	$-0.8^{+2.9}_{-2.5}$	1.00 ± 0.25
y (%)	0.81 ± 0.16	$0.7^{+2.4}_{-2.7}$	0.76 ± 0.18
$\delta_D^{K\pi}$	$-151.5^{+9.6}_{-9.5}$	-130^{+38}_{-28}	$-157.5^{+10.4}_{-11.0}$
$\mathcal{B}(D^0 \rightarrow K^-\pi^+)$ (%)	3.89 ± 0.05	3.89 ± 0.05	3.89 ± 0.05
$\mathcal{B}(D^0 \rightarrow K^+\pi^-)$ (10^{-4})	1.47 ± 0.07	1.47 ± 0.07	1.47 ± 0.07
$\mathcal{B}(D^0 \rightarrow K^-\pi^+\pi^0)$ (%)	13.8 ± 0.5	13.8 ± 0.5	13.9 ± 0.5
$\mathcal{B}(D^0 \rightarrow K^+\pi^-\pi^0)$ (10^{-4})	3.05 ± 0.17	3.05 ± 0.17	3.05 ± 0.17
$\mathcal{B}(D^0 \rightarrow K^-\pi^+\pi^+\pi^-)$ (%)	7.96 ± 0.19	8.03 ± 0.19	8.10 ± 0.20
$\mathcal{B}(D^0 \rightarrow K^+\pi^-\pi^-\pi^+)$ (10^{-4})	2.65 ± 0.19	2.63 ± 0.19	2.62 ± 0.20

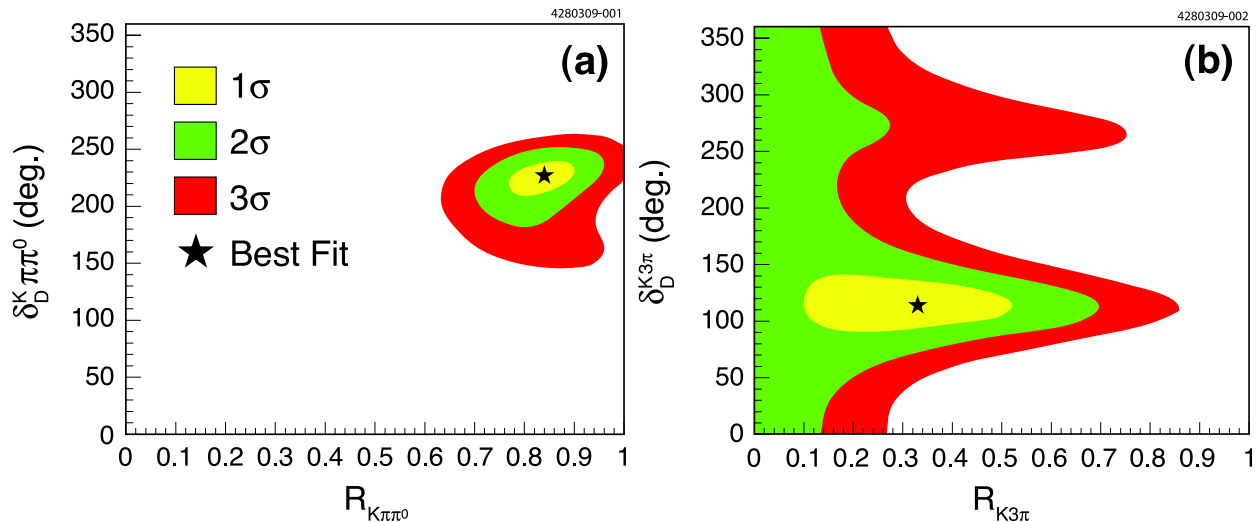


FIG. 2: The 1σ , 2σ and 3σ allowed regions of (a) $(R_{K\pi\pi^0}, \delta_D^{K\pi\pi^0})$ and (b) $(R_{K3\pi}, \delta_D^{K3\pi})$ parameter space.

rameters from the data; this procedure is referred to as the mixing-unconstrained fit. The Δ_{CP}^F observables are dependent on the value of $\delta_D^{K\pi}$ and its uncertainty from the normalisation method that used the measured values of $S(CP|K^-\pi^+)$. Therefore, initially the value and uncertainties of Δ_{CP}^F are recalculated assuming $\cos \delta_D^{K\pi} = 0 \pm 1$ and the mixing-unconstrained fit is performed. The resulting value of $\delta_D^{K\pi}$ is used to recalculate Δ_{CP}^F and the mixing-unconstrained fit is repeated. This procedure is iterated until the parameter values returned by the fit no longer changed within the quoted precision. The results of the final iteration are shown in Tab. V. The best-fit values of x , y , and $\delta_D^{K\pi}$ are: $x = (-0.8^{+2.9}_{-2.5})\%$,

$y = (-0.7_{-2.7}^{+2.4})\%$, and $\delta_D^{K\pi} = (-130_{-28}^{+38})$. There is an ambiguity in the solution of the unconstrained-fit if the signs of $\delta_D^{K\pi}$, $\delta_D^{K3\pi}$, $\delta_D^{K\pi\pi^0}$ and x are all reversed. The correlations amongst the fit parameters maybe found in Ref. [19].

In summary, the first determination of the coherence factors and average strong-phase differences for $D^0 \rightarrow K^-\pi^+\pi^0$ and $D^0 \rightarrow K^-3\pi$ has been presented. The results show significant coherence for $D^0 \rightarrow K^-\pi^+\pi^0$, but no significant coherence for $D^0 \rightarrow K^-3\pi$. These results will improve the measurement of the unitarity triangle angle γ and the amplitude ratio r_B in $B^- \rightarrow DK^-$ decays, where the D decays to $K^-\pi^+\pi^0$ and $K^-3\pi$. The preliminary result for $R_{K3\pi}$ and $\delta_D^{K3\pi}$ [20] combined with CLEO-c's measurement of $\delta_D^{K\pi}$ [10] was shown to improve the expected sensitivity to γ at LHCb in a combined ADS analysis of $K\pi$ and $K3\pi$ final states by up to 40% [21]. The sensitivity of these data to y and $\delta_D^{K\pi}$ is also presented.

We gratefully acknowledge the effort of the CESR staff in providing us with excellent luminosity and running conditions. This work was supported by the A.P. Sloan Foundation, the National Science Foundation, the U.S. Department of Energy, the Natural Sciences and Engineering Research Council of Canada, and the U.K. Science and Technology Facilities Council.

-
- [1] B. Aubert *et al.* (BABAR Collaboration), arXiv:0902.1708 [hep-ex]; K.-F. Chen *et al.* (Belle Collaboration), Phys. Rev. Lett. **98**, 031802 (2007).
 - [2] N. Cabibbo, Phys. Rev. Lett. **10**, 531 (1963); M. Kobayashi and T. Maskawa, Prog. Theor. Phys. **49**, 652 (1973).
 - [3] Here and throughout this letter the charge-conjugate state is implied unless otherwise stated.
 - [4] M. Gronau and D. London, Phys. Lett. B **253**, 483 (1991); M. Gronau and D. Wyler, Phys. Lett. B **265**, 172 (1991).
 - [5] D. Atwood, I. Dunietz and A. Soni, Phys. Rev. Lett. **78**, 3257 (1997); D. Atwood, I. Dunietz and A. Soni, Phys. Rev D **63**, 036005 (2001).
 - [6] A. Giri, Yu. Grossman, A. Soffer and J. Zupan, Phys. Rev. D **68**, 054018 (2003).
 - [7] E. Barberio *et al.* (Heavy Flavour Averaging Group), arXiv:0808.1297 [hep-ex] (2008).
 - [8] B. Aubert *et al.* (BABAR Collaboration), Phys. Rev. D **72**, 032004 (2005).
 - [9] Y. Horii *et al.* (Belle Collaboration), Phys. Rev. D **78**, 071901(R) (2008).
 - [10] D.M. Asner *et al.* (CLEO Collaboration), Phys. Rev. D **78**, 012001 (2008).
 - [11] C. Amsler *et al.* (Particle Data Group), Phys. Lett. B **667**, 1 (2008).
 - [12] D. Atwood and A. Soni, Phys. Rev. D **68**, 033003 (2003).
 - [13] For a review see M. Artuso, B. Meadows and A. A. Petrov, Ann. Rev. Nucl. Part. Sci. **58**, 249 (2008).
 - [14] Z.Z. Xing, Phys. Rev. D **55**, 196 (1997).
 - [15] Y. Kubota *et al.* (CLEO Collaboration), Nucl. Instrum. Methods Phys. Res., Sect. A **320**, 66 (1992); D. Peterson *et al.* (CLEO Collaboration), Nucl. Instrum. Methods Phys. Res., Sect. A **478**, 142 (2002); M. Artuso *et al.*, Nucl. Instrum. Methods Phys. Res., Sect. A **502**, 91 (2003); R.A. Briere *et al.* (CLEO-c/CESR-c Taskforces and CLEO-c Collaboration), Cornell LEPP Report CLNS Report No. 01/1742 (2001).
 - [16] S. Dobbs *et al.* (CLEO Collaboration), Phys. Rev. D **76**, 112001 (2007).
 - [17] Q. He *et al.* (CLEO Collaboration), Phys. Rev. Lett. **100**, 091801 (2008).

- [18] Differing definitions of the CP operation on a D^0 state between the formalism of charm-mixing measurements [7, 10] and the formalism in this Letter leads to a 180° phase shift to the measured value of $\delta_D^{K\pi}$ when used to extract the observables and parameters.
- [19] EPAPS addendum to paper.
- [20] A. Powell, arXiv:0805.1722 [hep-ex].
- [21] K. Akiba *et al.*, CERN-LHCb-2008-031 (2008).

EPAPS addendum

TABLE VI: Correlation matrix for the mixing-constrained fit. Only elements above the diagonal are shown.

	$\delta_D^{K3\pi}$	$R_{K\pi\pi^0}$	$\delta_D^{K\pi\pi^0}$	x	y	$\delta_D^{K\pi}$	\mathcal{B}_1	\mathcal{B}_2	\mathcal{B}_3	\mathcal{B}_4	\mathcal{B}_5	\mathcal{B}_6
$R_{K3\pi}$	-0.067	0.078	0.045	-0.082	-0.020	-0.014	0.002	0.008	0.071	0.325	-0.134	0.051
$\delta_D^{K3\pi}$	—	0.127	0.256	-0.008	0.140	0.188	-0.023	0.096	0.244	-0.031	-0.126	-0.032
$R_{K\pi\pi^0}$	—	—	0.455	0.080	-0.059	-0.046	-0.014	0.060	0.018	0.098	-0.138	0.150
$\delta_D^{K\pi\pi^0}$	—	—	—	-0.033	0.377	0.467	0.004	-0.027	0.142	0.131	-0.295	0.114
x	—	—	—	—	-0.189	-0.188	-0.001	0.005	-0.037	0.001	0.047	-0.006
y	—	—	—	—	—	0.945	0.004	-0.015	0.107	-0.014	-0.146	0.012
$\delta_D^{K\pi}$	—	—	—	—	—	—	0.005	-0.004	0.121	-0.002	-0.071	0.008
\mathcal{B}_1	—	—	—	—	—	—	—	0.006	-0.005	0.008	0.001	-0.002
\mathcal{B}_2	—	—	—	—	—	—	—	—	0.005	-0.028	-0.024	0.008
\mathcal{B}_3	—	—	—	—	—	—	—	—	—	0.104	0.047	-0.001
\mathcal{B}_4	—	—	—	—	—	—	—	—	—	—	-0.054	-0.006
\mathcal{B}_5	—	—	—	—	—	—	—	—	—	—	—	0.028

Key of branching fractions (\mathcal{B}):

$$\mathcal{B}_1 \equiv \mathcal{B}(D^0 \rightarrow K^- \pi^+)$$

$$\mathcal{B}_2 \equiv \mathcal{B}(D^0 \rightarrow K^+ \pi^-)$$

$$\mathcal{B}_3 \equiv \mathcal{B}(D^0 \rightarrow K^- \pi^+ \pi^+ \pi^-)$$

$$\mathcal{B}_4 \equiv \mathcal{B}(D^0 \rightarrow K^+ \pi^- \pi^- \pi^+)$$

$$\mathcal{B}_5 \equiv \mathcal{B}(D^0 \rightarrow K^- \pi^+ \pi^0)$$

$$\mathcal{B}_6 \equiv \mathcal{B}(D^0 \rightarrow K^+ \pi^- \pi^0)$$

TABLE VII: Correlation matrix for the mixing-unconstrained fit. Only elements above the diagonal are shown.

	$\delta_D^{K3\pi}$	$R_{K\pi\pi^0}$	$\delta_D^{K\pi\pi^0}$	x	y	$\delta_D^{K\pi}$	\mathcal{B}_1	\mathcal{B}_2	\mathcal{B}_3	\mathcal{B}_4	\mathcal{B}_5	\mathcal{B}_6
$R_{K3\pi}$	-0.093	-0.293	-0.546	-0.558	-0.175	-0.505	0.002	0.009	0.038	0.245	-0.079	0.069
$\delta_D^{K3\pi}$	—	0.763	-0.179	0.577	-0.819	0.012	-0.002	0.014	0.231	-0.166	-0.121	-0.045
$R_{K\pi\pi^0}$	—	—	-0.049	0.802	-0.596	-0.108	-0.005	0.028	0.058	-0.124	-0.006	0.029
$\delta_D^{K\pi\pi^0}$	—	—	—	0.175	0.504	0.692	0.002	-0.026	0.194	-0.003	-0.308	0.034
x	—	—	—	—	-0.232	0.092	0.003	-0.003	0.035	-0.132	0.072	-0.042
y	—	—	—	—	—	0.255	-0.004	0.015	-0.081	0.144	0.029	0.008
$\delta_D^{K\pi}$	—	—	—	—	—	—	0.006	-0.034	0.211	-0.157	-0.223	-0.038
\mathcal{B}_1	—	—	—	—	—	—	—	0.005	-0.003	0.006	-0.000	-0.002
\mathcal{B}_2	—	—	—	—	—	—	—	—	-0.007	-0.018	-0.012	0.008
\mathcal{B}_3	—	—	—	—	—	—	—	—	—	0.075	-0.013	0.000
\mathcal{B}_4	—	—	—	—	—	—	—	—	—	—	-0.017	-0.005
\mathcal{B}_5	—	—	—	—	—	—	—	—	—	—	—	0.017